

Searching for New Microbiome-Targeted Therapeutics through a Drug Repurposing Approach

Monica Barone,[#] Simone Rampelli,[#] Elena Biagi, Sine Mandrup Bertozzi, Federico Falchi, Andrea Cavalli, Andrea Armirotti, Patrizia Brigidi, Silvia Turroni, and Marco Candela*Cite This: *J. Med. Chem.* 2021, 64, 17277–17286

Read Online

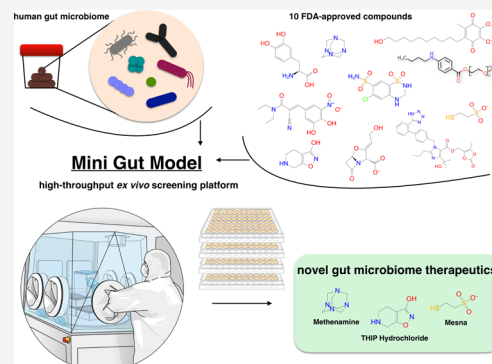
ACCESS |

Metrics & More

Article Recommendations

Supporting Information

ABSTRACT: Commonly used non-antibiotic drugs have been associated with changes in gut microbiome composition, paving the way for the possibility of repurposing FDA-approved molecules as next-generation microbiome therapeutics. Herein, we developed and validated an *ex vivo* high-throughput screening platform—the mini gut model—to underpin human gut microbiome response to molecular modulators. Ten FDA-approved compounds, selected based on maximum structural diversity of molecular fingerprints, were screened against the gut microbiome of five healthy subjects to characterize the ability of human-targeted drugs to modulate the human gut microbiome network. Three compounds, THIP hydrochloride, methenamine, and mesna, have shown promise as novel gut microbiome therapeutics in light of their capability of promoting health-associated features of the gut microbiome. Our findings provide a resource for future research on drug–microbiome interactions and lay the foundation for a new era of more precise gut microbiome modulation through drug repurposing, aimed at targeting specific dysbiotic events.



INTRODUCTION

The human gut microbiome (GM) plays a central role in our health as virtually no part of human physiology is untouched by commensal microorganisms.¹ The GM is indeed strategic for the correct functionality of our metabolic and immune systems and, in parallel, seems to regulate functions of the central nervous system, endocrine system, and bone marrow.² The GM centrality for human biology is also highlighted by the number of chronic diseases associated with an unbalanced GM layout, ranging from inflammatory and metabolic conditions to neurological, cardiovascular, and respiratory diseases.³ The connection between a dysbiotic GM and multiple diseases has made the microbiome a strategic therapeutic target, paving the way for the development of a series of microbiome-tailored intervention strategies aimed at rehabilitating a health-promoting layout.^{4–6} However, current approaches for GM modulation lack selectivity and exhibit limited efficacy, being very rudimentary compared to other pharmaceutical therapeutic products.⁷ For instance, probiotics and prebiotics are relatively safe but not particularly powerful in terms of modifying the overall GM structure and with limited impact on disease symptoms.⁸ Fecal microbiota transplantation is approved for the treatment of *Clostridioides difficile*-associated diarrhea and shows promising preliminary results for other GM-related disorders. However, transplanting an entire microbial community carries potential risks in terms of pathogen transfer, adverse effects, and long-term stability.⁷

In this current scenario, with a view to develop a narrow spectrum of next-generation microbiome modulators to more precisely alter human GM, the possibility of shaping the overall GM structure by administering bioactive molecules has been advanced.^{4,5,7,9} In particular, since drugs designed to target human cells have recently been demonstrated to interfere with GM metabolism,^{10,11} the possibility of repurposing FDA-approved molecules as next-generation microbiome therapeutics has been suggested.^{9,12}

To identify potential next-generation microbiome modulators, here we *in silico* parsed the FDA-approved drug database with the aim of selecting a limited number of compounds (10 molecules) covering the largest possible chemical diversity. Notably, we removed from the selection all compounds with known antibacterial activity as they have been reported to impact GM as one of the major side effects of therapy with this drug family. Hence, to assess whether and how these compounds modified human GM, we exploited an original *ex vivo* minimal model (the mini gut model—MGM). Essentially, our MGM consisted of miniaturized batch cultures

Received: July 28, 2021

Published: November 30, 2021



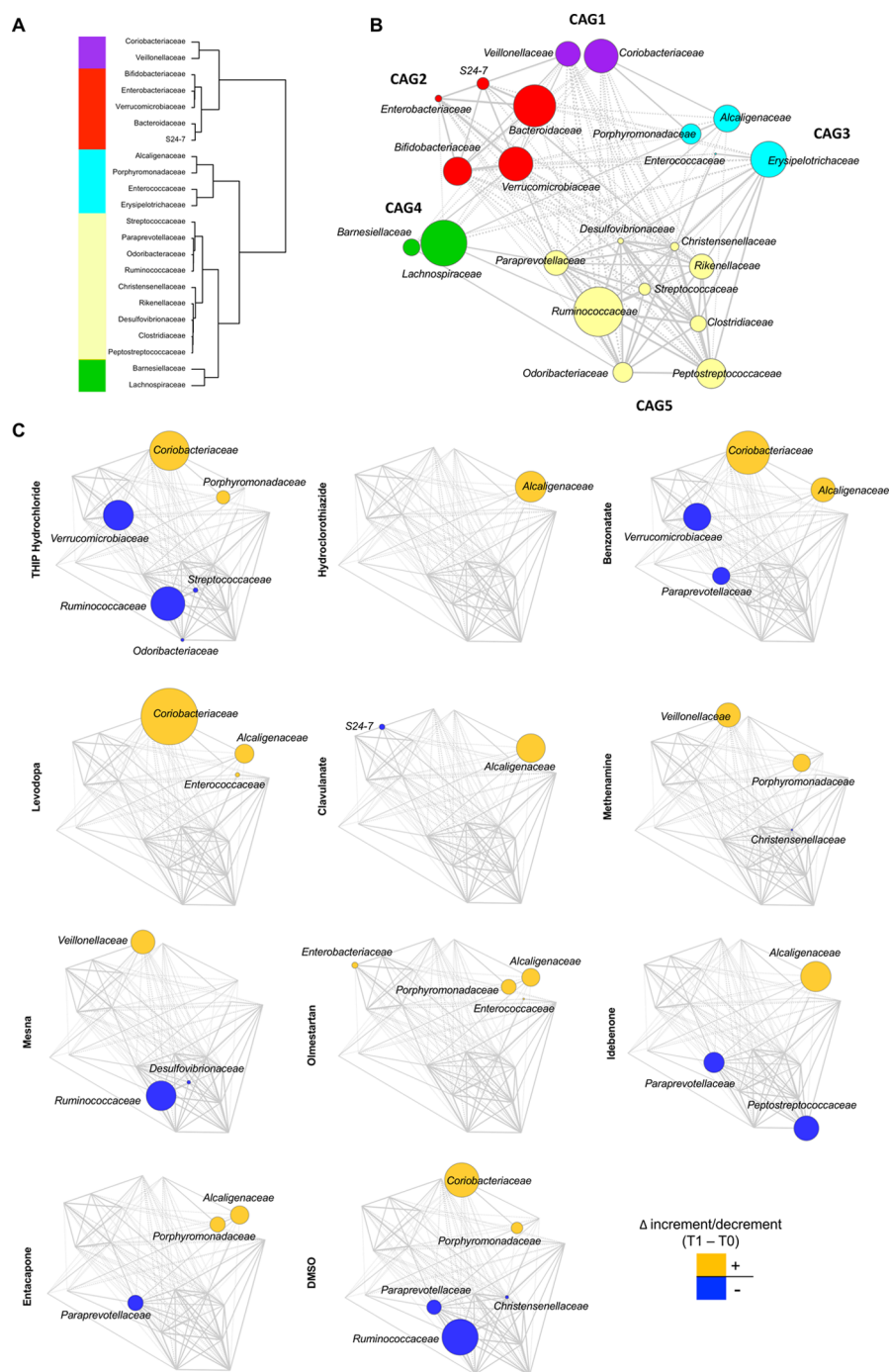


Figure 1. The 10 FDA-approved compounds modulate different GM components in MGMs. (A) Co-abundance group (CAG) assignment relied on a hierarchical clustering based on Kendall correlations between families clustered by the Spearman correlation coefficient and Ward linkage. The core microbiome, constituted by dominant bacterial families (*i.e.*, with relative abundance >0.1% and sample prevalence of at least 20%), was selected for this analysis. Colors are indicative of the five identified CAGs. (B) Wiggum plot correlations between the five CAGs identified. Circle size is proportional to the mean relative abundance of the bacterial families at T0, and the connections between nodes represent significant Kendall correlations between families ($FDR \leq 0.05$; positive correlations with solid lines, negative correlations with dotted lines). (C) Wiggum plots showing the specific effects of the 10 compounds on the GM structure at T1. Disk sizes indicate variations (increment/decrement) in the relative abundances of bacterial families (T1–T0). Only variations >20% with respect to T0 and in any case higher than 0.2% of relative abundance were displayed.

of GM in an mGAM medium,^{11,13,14} inoculated with freshly collected fecal slurries stable for up to 48 h under anaerobic conditions. Variations in compositional structure and active fraction of GM in the MGM were assessed using a combined next-generation sequencing-based approach, merging 16S rRNA gene sequencing and metatranscriptomics. According

to our data, the selected compounds, which have not previously been reported to impact GM, are able to modify human GM to varying degrees, both qualitatively and quantitatively, showing that it is possible to reposition FDA-approved drugs as next-generation therapeutics targeting human GM. Additionally, the present study paves the way

for innovative drug discovery programs purposely conceived to identify novel compounds able to specifically modulate human GM, thus opening up new avenues to treat unmet medical needs in which altered GM plays a major role.

RESULTS

Setup and Validation of the Mini Gut Model of the Human GM. In order to evaluate the impact of 10 FDA-approved small molecules on human GM, we set up an MGM screening platform, essentially consisting of an *ex vivo* array of 96-well fermentation reactions inoculated with stools (Figure S1). In particular, the miniaturized batch cultures were inoculated with freshly produced stools diluted 1:100 in 0.5 mL of pre-reduced mGAM medium. Incubation was performed at 37 °C under an atmosphere of 5% H₂, 10% CO₂, and 85% N₂ inside an anaerobic workstation for up to 48 h. With the aim of testing the reliability of our MGM system as an *ex vivo* model of human GM, we inoculated 36 MGM wells with freshly produced stools from two healthy donors, monitoring bacterial growth by measuring optical density (OD) immediately after inoculation as well as after 24 and 48 h of fermentation (six technical replicas per time point). The increase in OD observed after 24 h (log₂ fold change, mean ± SD, 0.76 ± 0.044) indicates effective bacterial growth within the MGM. On the other hand, the slight decrease observed after 48 h of fermentation reflects the overcoming of the typical peak observed in the exponential phase of microbial growth, suggesting the achievement of the plateau phase. GM variation within the MGM was monitored by 16S rRNA gene sequencing. To this aim, samples were collected at the inoculum and following 24 and 48 h of incubation. A total of 989,708 high-quality sequences (mean ± SD, 27,491 ± 5110 sequences per sample) were obtained and subsequently binned into 2746 high-resolution ASVs (amplicon sequence variants). Alpha diversity throughout the whole fermentation process was assessed by means of the phylogenetic metrics PD whole tree and Shannon and Simpson indices and by evaluating the total ASV count (Figure S2). Our results suggest the preservation of a level of biodiversity well approximating the *in vivo* condition throughout the entire process (*P*-value ≥ 0.05, Wilcoxon test). The composition of the microbial ecosystem at the genus level also did not vary significantly over time for either donor (*P*-value ≥ 0.05, Wilcoxon test). A significant positive correlation was indeed found between the genus-level MGM microbial profiles after the inoculum and 24 or 48 h of fermentation, highlighting an overall correspondence of GM structures over time (Kendall correlation test, *P*-value ≤ 7.1 × 10⁻⁴, tau ≥ 0.44) (Figure S2). Our results are in line with what was previously observed by Maier et al.¹¹ and Tramontano et al.,¹⁴ confirming the efficiency of mGAM in closely mimicking the growth conditions in terms of nutrients used by bacteria in the human gut, supporting the *ex vivo* stability and growth of human gut-derived microbial cells for up to 48 h within our high-throughput screening platform.

Selection of 10 Compounds as Potential Human GM Modulators and Assessment of GM Modulation Activity in the MGM. The compounds in this work were selected from the Prestwick Chemical Library. This library consists of 1280 off-patent small molecules, 95% approved drugs (FDA, EMA, and other agencies) selected for the high chemical and pharmacological diversity and for the known bioavailability and safety in humans. To reduce the number of compounds, first of

all, we discarded antibacterial drugs, for which an overall impact in terms of reduction of the total GM diversity is expected. After that, 10 compounds were selected on the basis of the maximum structural diversity described in terms of molecular fingerprints.

For the screening of the GM modulation activity of the 10 selected compounds, freshly prepared fecal slurries from five healthy human donors were used to inoculate 330 MGMs, 66 per subject. In particular, for each donor, three MGMs (biological replicates) were incubated with 20 μM each of the 10 selected FDA-approved compounds or with the vehicle (DMSO) as a control. A concentration of 20 μM was selected as below the median small intestine and colon concentration of human-targeted drugs.^{11,15} Samples were collected from MGMs at two time points: inoculum (T0) and after 24 h (T1), *i.e.*, before reaching the stationary phase. During the fermentation process, microbial growth was monitored by OD measurement (Figure S3). At T0 and T1, the GM was assessed by 16S rRNA gene sequencing to provide insights into the ecosystem layout. A total of 11,530,996 high-quality sequences, with an average of 34,942 ± 25,542 reads per sample, were obtained and clustered into 28,061 high-resolution ASVs. The levels of intra-sample diversity were overall maintained throughout the entire fermentation process, even in the presence of the selected FDA-approved compounds (*P*-value = 0.083, Kruskal–Wallis test; Figure S3). In order to identify patterns of GM variation in response to the selected compounds, we chose to apply a network modeling approach to reduce the degree of complexity. The idea behind our reductional approach was first to build the GM network at T0 and then to evaluate the activity of the compounds in terms of modulation of the GM network structure at T1. To this aim, co-abundance associations between GM families were first extracted from the whole dataset, resulting in five co-abundance groups (CAGs 1–5) (Figure 1A). Next, the topological structure of the human GM network at T0 was constructed and represented by a Wiggum plot (Figure 1B). The GM response to the different compounds was then assessed in terms of changes in the network structure at T1, expressed as the variation in the relative abundance of the constituent CAGs members. In particular, as a parsimonious approach, for a given GM family, we considered a relevant positive (or negative) variation when the corresponding increase (or decrease) in relative abundance at T1 doubled its standard deviation at T0, in at least four out of five analyzed subjects. In Figure 1C, for each of the selected compounds, we provide the Wiggum plot representing, for each CAG, the corresponding families for which a positive or negative variation at T1 was found. According to our findings, of the five detected CAGs, only one, CAG 5, was not affected by the selected compounds. Generally, CAGs 1 and 3 were positively affected, while CAGs 2 and 4 were negatively affected. Interestingly, each CAG showed a compound-specific response in terms of positively or negatively modulated families, as shown in Table S1. In terms of overall GM modulation activity, the 10 compounds resulted in a specific network modulation pattern, different from that obtained with the compound vehicle, which alone resulted in the reduction of Ruminococcaceae and the increase in Coriobacteriaceae, among other minor effects. Among the tested compounds, THIP hydrochloride, methenamine, and mesna showed promising and specific GM modulation activity. In particular, THIP hydrochloride was the only compound that led to the

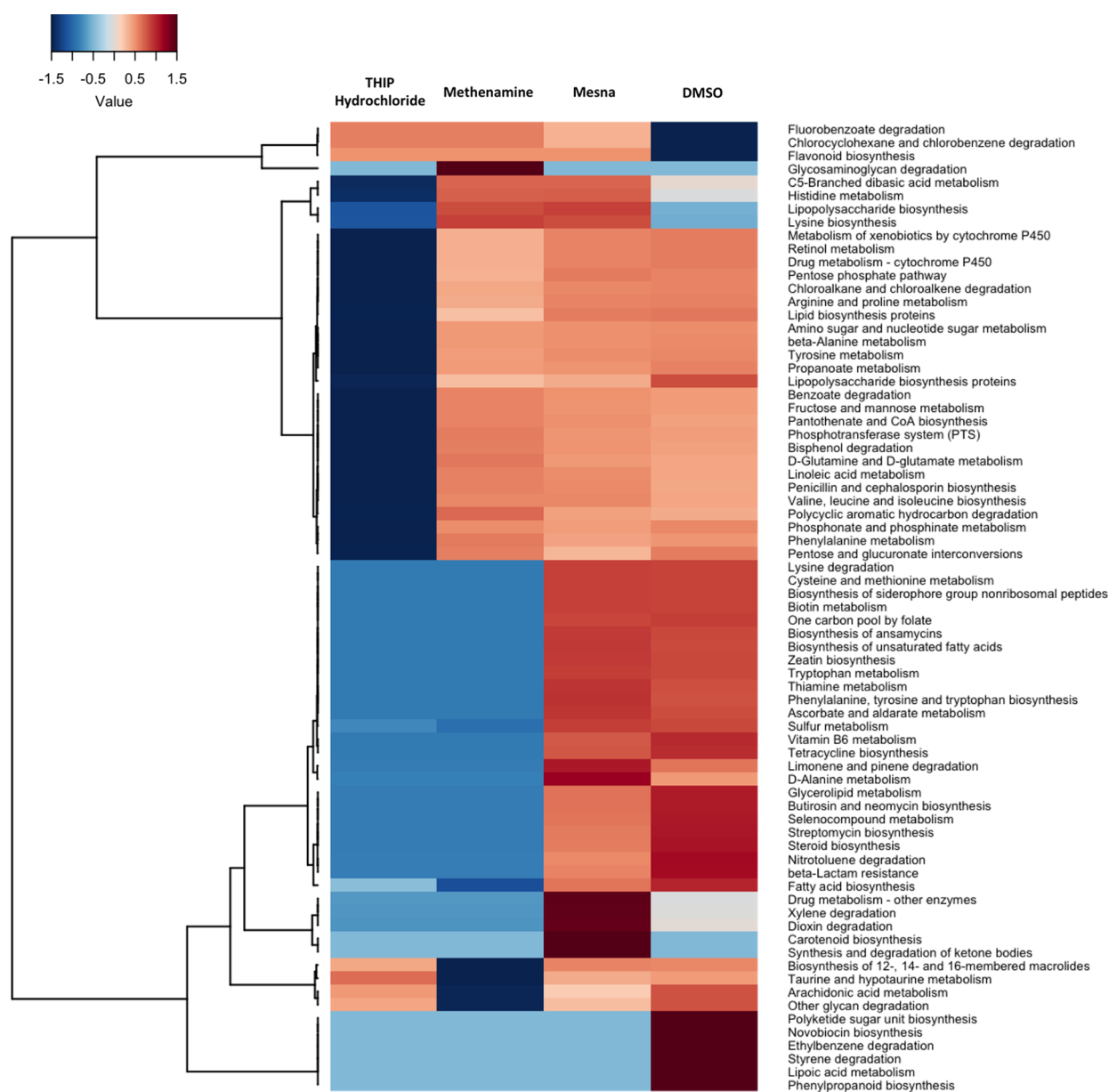


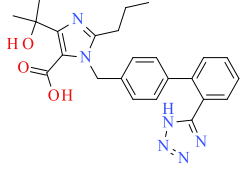
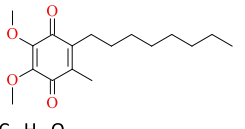
Figure 2. Small molecules' impact on the expression levels of KEGG categories within MGMs. Bi-clustering of \log_2 fold changes (T1/T0) of 73 KEGG categories whose gene expression was most affected by 24h of incubation with at least one compound (*i.e.*, THIP hydrochloride, methenamine, and mesna), clustered by Ward's method for both KEGG categories (rows) and compounds (columns).

reduction of Verrucomicrobiaceae and Streptococcaceae, while methenamine and mesna were both characterized by the enhancement of Veillonellaceae. For mesna, the reduction of Desulfovibrionaceae was also observed as a compound-specific effect. Finally, we cannot fail to mention that several of the GM network modulation activities observed for the selected compounds were actually shared and thus probably attributable to the DMSO vehicle, mainly the reduction of Ruminococcaceae and the increase in Coriobacteriaceae.

Metatranscriptomic Analysis Reveals the Ability of THIP Hydrochloride, Methenamine, and Mesna to Influence Community-Wide Gene Expression. For THIP hydrochloride, methenamine, mesna—as well as for the DMSO vehicle—MGM screening readouts from donor 1 were further assessed by transcriptomic shotgun sequencing (RNA-seq), allowing for whole-genome analysis of the metatranscriptome under the different MGM experimental

conditions. Similar to 16S rRNA gene sequencing, RNA-seq profiles were obtained immediately after MGM inoculation (T0) and 24 h (T1) of incubation with each of the selected compounds. The shotgun sequencing yielded a total of 3,840,057 high-quality paired-end reads. For each of the selected compounds, we explored the impact on the GM ecosystem in terms of changes in the transcriptional profile of community-wide KEGG pathways from T0 to T1. Gene expression of 73 KEGG pathways was affected by 24 h of incubation with at least one compound (\log_2 fold change threshold, ± 2) (Table S2). These pathways mainly included those involved in carbohydrate and amino acid metabolism as well as several functionalities involved in xenobiotics biodegradation and the biosynthesis of secondary metabolites. The latter data are indicative of a general transcriptome response involving functionalities related to stress response. In Figure 2, we provide a bi-clustering of the \log_2 fold change of

Table 1. Summary of the Transformations Observed for the 10 Compounds under Investigation

Group	Drug Name	Estimated Half-life $t_{1/2}$ (h)	Observed metabolism or degradation product(s)	Metabolism data reported in DrugBank ^a
1 Stable in all conditions	Hydrochlorothiazide	>48	None	Not metabolized (DB00999)
	Benzonatate	>48	None	Hydrolysis to PABA (DB00868)
2 Unstable in reference incubation	Olmesartan	n.a. ^b	 C ₂₄ H ₂₇ N ₆ O ₃ (loss of medoxomil)	Rapid and complete ester hydrolysis to active drug (DB00275)
	Mesna	-	Dismesma	Immediate oxidation to Dismesna (DB09110)
	Clavulanate potassium salt	-	No metabolites detected ^c	No data (DB00766)
	THIP Hydrochloride	-	No metabolites detected ^c	No data (DB06554)
3	Entacapone	~12	Isomerization; No glucuronidation	Isomerization and glucuronidation of both parent and isomer (DB00494)
	Idebenone	~12	 C ₁₇ H ₂₆ O ₄ (loss of -CH ₂ -CH ₂ -O-)	Oxidative shortening of the side chain, reduction of the quinone ring and conjugation to the corresponding glucuronides and sulfates (DB09081)
	Methenamine	10	No metabolites detected ^c (CH ₂ O and NH ₃)	Hydrolysis to formaldehyde and ammonia under acidic conditions (DB06799)
	Levodopa	30	No metabolites detected ^c	Conversion to dopamine or 3-O-methyldopamine and their corresponding sulfated and glucuronidated conjugates (DB01235)

^aThe literature references are indicated as reported in the corresponding DrugBank entry. ^bn.a. = not available. ^cNo metabolites or degradation products confidently identified in the analytical setup used (very low MW or volatile compounds formed).

the transcriptional values at T1 for each of the tested compounds (and DMSO). This analysis allowed highlighting two pathways involved in xenobiotic degradation, specifically activated by the three tested compounds, while being downregulated by the vehicle alone, *i.e.*, fluorobenzoate degradation and chlorocyclohexane and chlorobenzene degradation. Furthermore, methenamine and mesna resulted in the overrepresentation of other specific pathways involved in xenobiotic and drug metabolism. In contrast, THIP hydrochloride resulted in the underrepresentation of a cluster of pathways including a vast range of functionalities, from carbohydrate and amino acid metabolism to metabolism of cofactors and vitamins.

Biotransformation of Selected Compounds. We tested the chemical and metabolic stability of the compounds under investigation by incubating them both in mGAM itself (free of bacteria) and in the presence of the GM from donor 1 in MGMs for up to 24 h. For this purpose, we targeted the parent compound and measured its decay over time. Benzonatate and hydrochlorothiazide showed marked stability to both chemical and metabolic actions from both mGAM and GM components: no detectable levels of degradation products or metabolites were observed in our experiments. On the other hand, four compounds (olmesartan, mesna, clavulanate, and

THIP hydrochloride) showed a marked instability under the conditions of the assay itself (reference incubation): at 24 h, they were virtually absent in the medium alone, in the absence of bacteria. Conversely, entacapone, idebenone, methenamine, and levodopa were clearly degraded only in the presence of human GM, while remaining stable under the assay conditions. For all the compounds under investigation, high-resolution LC-MS/MS was used to identify the observed degradation products or metabolites. The obtained data were then compared with the reference information reported in the DrugBank database (<https://www.drugbank.ca/>). Table 1 shows the results of the transformations observed for all the tested compounds. It is important to point out that mGAM was *per se* a very aggressive medium for these compounds as 14% of its composition (in weight) consists of yeast, meat, and liver extracts. This is why, most likely, the metabolites that we confidently identified in our experiments correspond to metabolites of these compounds known to be produced in humans by phase 1 metabolism. In this regard, the MGM herein developed partially mimics the natural digestion process of food, with compounds undergoing a phase 1-like metabolism before being exposed to bacterial metabolism (see for example olmesartan).

DISCUSSION

Here, we developed and validated an MGM-based approach for high-throughput *ex vivo* screening of the GM response to molecular modulators, bioactive small molecules, and stressors of different types, such as potential prebiotic molecules, drugs, and xenobiotics. MGMs were proven to support *ex vivo* stability and growth of human GM for up to 48 h as demonstrated by the maintenance of a level of biodiversity and ecosystem compositional structure comparable to those observed in inoculum after 24 and 48 h of incubation. The *ex vivo* “lifetime” of MGMs is sufficient to observe a GM dynamic response to a given input as demonstrated by David and colleagues¹⁶ under real-life conditions, where GM variations to host dietary changes were shown to occur within 24 h. Specifically, in our work, MGMs were used to screen for new potential microbiome-targeted therapeutics through a drug repurposing approach. For this aim, 10 compounds from the Prestwick Chemical Library were selected. Compounds were selected for spanning a wide range of chemical and pharmacological diversity as well as for the known bioavailability and safety in humans. A detailed description of the compounds’ therapeutic profile is provided in the [Supporting Information](#).

To screen for the GM modulation activity of the 10 selected compounds, MGMs were inoculated with stools from five healthy donors aged 25–35 years. Based on our findings, all the tested compounds showed the potential to modulate the human GM network at a concentration consistent with the median small intestine and colon concentration of human-targeted drugs. In particular, each compound prompted a specific reconfiguration of the human GM network topology, targeting a peculiar set of constituent bacterial families, with an overall pattern different from that observed with the drug vehicle alone. Interestingly, four out of the five CAGs that were identified in the human GM were modulated by at least one of the selected compounds. This demonstrates the possibility of selectively targeting the great majority of the different human GM hubs (*i.e.*, modules of highly interconnected microorganisms in the network topology), covering all the main human GM components. Among the 10 tested compounds, THIP hydrochloride, methenamine, and mesna exhibited human GM modulatory properties with specificities suggesting their potential to be implemented as microbiome therapeutics to target specific dysbiotic events. In particular, THIP hydrochloride was shown to specifically reduce members of the Verrucomicrobiaceae family, including *Akkermansia muciniphila*. Due to its mucin-degrading capacity, the overgrowth of this microorganism has been linked to potentially severe damage of the colonic mucosa and consequently extensive endotoxin leakage, ultimately being involved in several pathological circumstances, such as multiple sclerosis and Parkinson’s disease.^{17–19} A reduction of its relative abundance could therefore be strategic under certain conditions to recover intestinal eubiosis. Conversely, methenamine specifically boosted Veillonellaceae, a lactate-utilizing family that has been demonstrated to provide beneficial functions under stress and intense physical activity.²⁰ Finally, mesna jointed two interesting activities, boosting Veillonellaceae and, in parallel, reducing Desulfovibrionaceae, a pro-inflammatory GM component that, through the production of endotoxins and H₂S, has been associated with several dysbiosis-related diseases, such as inflammatory bowel disease

and autism spectrum disorders.^{21–24} For these three promising compounds, the impact on the human GM was further explored by analyzing changes in the overall transcriptional profile. According to our findings, the three compounds were able to shape the GM metatranscriptome, suggesting an active interaction with the overall GM metabolism. In particular, all of them led to the upregulation of specific patterns of functionality involved in xenobiotic biodegradation, biosynthesis of secondary metabolites, and lipid and amino acid metabolism, underlining an adaptive GM response to the presence of xenobiotics. When we explored the fate of the 10 selected compounds following incubation in MGMs, a marked stability to chemical and metabolic actions by both the medium (mGAM) and GM components was observed for benzonatate and hydrochlorothiazide. Differently, olmesartan, mesna, clavulanate, and THIP hydrochloride showed a relevant instability in mGAM, disappearing from the medium even in the absence of bacteria. Finally, entacapone, idebenone, methenamine, and levodopa were clearly degraded only in the presence of human GM. Taken together, these data demonstrate that, depending on the stability of the molecules in the human gastrointestinal tract, the different compounds can directly interact with the human GM or following phase 1 and 2 metabolism.

In conclusion, with our work, we provide preliminary experimental evidence of the possibility of targeting the human GM with selected small compounds, resulting in specific changes in ecosystem configuration and functionality. These findings may pave the way for a new era of more precise GM modulation, in which select molecular approaches can be implemented to specifically hit distinct dysbiotic layouts. By means of our repurposing approach, we were able to identify three candidate microbiome-targeting drugs, capable of modeling the human GM structure by favoring certain health-promoting characteristics. Although these compounds cannot yet be proposed as reliable microbiome therapeutics, our data might support a wider screening of FDA-approved molecules to be tested in MGMs inoculated with feces from a larger number of subjects of different ages and disease settings. The best-performing compounds can be selected, and the molecular mechanism of GM modulation can be dissected, allowing extrapolation of general principles to be used for the rational design of new molecular compounds for the precise restructuring of dysbiotic human GM layouts.

EXPERIMENTAL SECTION

General. Five healthy subjects provided a self-collected stool sample for *ex vivo* drug screening on active GM. Exclusion criteria included the following: age below 18 and over 65 years; BMI: <18.5 and >24.9 kg/m²; habitual intake of drugs and nutritional and pharmacological supplements of pre- and probiotics; taking antibiotics in the last 3 months; presence of intestinal and metabolic disorders (*i.e.*, inflammatory bowel disease, bacterial contamination syndrome, irritable bowel syndrome, constipation, celiac disease, type 1 and 2 diabetes, cardio- and neurovascular diseases, rheumatoid arthritis, allergies, neurodegenerative diseases, and cancer). Stools were used to inoculate our MGM platform to evaluate the effect of 10 FDA-approved small molecules after 24 and 48 h of fermentation. A combined method merging 16S rRNA gene sequencing and metatranscriptomics was used to evaluate GM structure and functional variations related to co-incubation with the selected compounds. DNA and RNA were extracted from all samples and subsequently sequenced on an Illumina MiSeq (for 16S rRNA gene amplicons) and NextSeq (for total mRNA) platform, respectively. Furthermore, the production of metabolites was evaluated along the

fermentation process to assess the microbial biotransformation potential of the selected compounds. These analyses are detailed in the following sections. All work was approved by the Ethics Committee of the Sant'Orsola-Malpighi Hospital, University of Bologna (ref. number: 118/2015/U/Tess).

Compound Selection. The Prestwick Chemical Library was obtained from Prestwick Chemical Inc. (Illkirch). To select the compounds used in the work, the 2D electronic Prestwick Chemical database (as an .sdf file) was cleaned up from all the compounds known to exert antibacterial activities. After that, the database was described in terms of molecular MOLPRINT 2D fingerprints using Canvas (Schrödinger Release 2016-4).^{25,26} The fingerprints were calculated at 64-bit precision. Ten compounds were selected with the maximum diversity between each other. Diversity was ensured by means of the "Selecting Diverse Structures" tool of canvas using "sphere" as the diversity selection method and Tanimoto as Metric. All compounds are >95% pure by HPLC analysis.

MGM Experimental Setup and Sample Processing. Freshly discharged fecal samples were collected from five healthy adult volunteers meeting inclusion criteria. In particular, no one had consumed pre- or probiotics the week before the donation, reported bowel symptoms in the past 3 months, or used medications in the last 2 weeks. Stool samples were transferred into an anaerobic chamber (Ruskinn) within 5 min of collection and homogenized in a pre-reduced mGAM medium (HyServe) and 10 mL/g feces. The obtained fecal slurry was let to stand for 5 min to allow large insoluble particles to settle. Fifty microliters of suspension was aliquoted into the MGM, consisting of 96 deep-well plates filled with 450 μ L of pre-reduced mGAM and incubated at 37 °C under an atmosphere of 5% H₂, 10% CO₂, and 85% N₂ inside the anaerobic workstation for up to 48 h. A correlation test performed on the genus-level dataset highlighted a significant positive correlation between stool samples and the respective fecal slurry (three biological replicates; P -value = 4.09×10^{-13} , $\tau = 0.484$; Kendall correlation test; donor 1), confirming the ability of the latter to reliably represent the composition of the stool sample and its suitability for use as a starting material for *ex vivo* drug screening with MGMs.

For compound screening experiments, 1 μ L of each drug (20 μ M, dissolved in DMSO) or vehicle (DMSO, used as blank) was mixed with fecal slurry in each well of the MGM screening platform containing 450 μ L of mGAM medium. The final DMSO concentration in the experimental condition was 0.22%. The mini-batch fermentations were conducted at 37 °C inside the anaerobic workstation for up to 48 h. MGM wells inoculated with selected compounds (without human GM) were used as a blank to separate the effects of drug metabolism by microbes from metabolic activity attributable to the mGAM medium alone. Each fermentation condition was carried out in triplicate to assess the reproducibility of the MGM screening platform. Kendall correlation tests showed limited experimental variation in microbial composition under controlled laboratory conditions (P -value $\leq 4.24 \times 10^{-5}$, $\tau \geq 0.60$).

Microbial growth within MGMs was monitored immediately after setting up the different fermentation conditions as well as after 24 and 48 h of *ex vivo* fermentation. Collected samples were diluted in mGAM, and OD₆₀₀ was measured using a spectrophotometer (Jasco).

Two hundred microliters of bacterial suspension were collected from each MGM well at three time points (0, 24, and 48 h), and microbial cells were pelleted through centrifugation at 8000g for 10 min at 4 °C. Pellets were used for 16S rRNA gene sequencing and metatranscriptomic analysis, and supernatant were used for metabolite analysis.

DNA Extraction and 16S rRNA Gene Sequencing. Microbial DNA was extracted from MGM pellets using the bead-beating plus column method²⁷ with the additional steps reported by Barone and colleagues.²⁸ Briefly, the pellets obtained from 200 μ L of bacterial suspension were suspended in 1 mL of lysis buffer (500 mM NaCl, 50 mM Tris-HCl pH 8, 50 mM EDTA, 4% [w/v] SDS), added with 0.5 g of 0.1 mm zirconia beads (BioSpec Products) and four 3 mm glass beads, and homogenized using the FastPrep instrument (MP Biomedicals) with 3 \times 1 min bead-beating steps at 5.5 m/s. After

incubation at 95 °C for 15 min and centrifugation at 13,000 rpm for 5 min, the nucleic acids were precipitated by adding 260 μ L of ammonium acetate and one volume of isopropanol. The pellets were then suspended in TE buffer. Removal of RNA and protein was performed by treatment with 2 μ L of DNase-free RNase (10 mg/mL) at 37 °C for 15 min and 15 μ L of proteinase K at 70 °C for 10 min. DNA purification was performed on silica columns following the manufacturer's instructions (QIAGEN). A NanoDrop ND-1000 spectrophotometer (NanoDrop Technologies) was used to quantify the purified DNA.

The V3-V4 hypervariable region of the 16S rRNA gene was PCR-amplified using the 341F and 785R primers with Illumina overhang adapter sequences, as previously reported.²⁸ Indexed libraries were prepared by limited-cycle PCR using Nextera technology, and the final library was diluted to 6 pM with 20% PhiX control. Sequencing was performed on an Illumina MiSeq platform using a 2 \times 250 bp paired-end protocol, according to the manufacturer's instructions. Sequencing data are available at NCBI SRA under the BioProject ID PRJNA749928.

RNA Extraction and Metatranscriptome Sequencing. The three replicate samples for each drug screening at each time point (0, 24, and 48 h) were pooled into one sample prior to microbial cell precipitation so as to have a representative sample of fermentation. Microbial RNA was extracted using the RNeasy PowerMicrobiome kit (QIAGEN), according to the manufacturer's instructions with minor adjustments. In particular, the homogenization step was performed using a FastPrep instrument (MP Biomedicals), with one treatment at 5.5 movements/sec for 1 min. For each sample, rRNA was depleted using the Ribominus Bacteria Transcriptome Isolation Kit (Invitrogen Life Technologies). RNA libraries were prepared using the QIAseq Stranded Total RNA Lib Kit (QIAGEN), according to the manufacturer's instructions, and pooled at an equimolar concentration of 4 nM. Sequencing was performed on an Illumina NextSeq 500 platform using a 2 \times 150 bp paired-end protocol, following the manufacturer's instructions. Sequencing data are available at NCBI SRA under the BioProject ID PRJNA759750.

Bioinformatics and Biostatistics. 16S rRNA gene sequences were processed using a pipeline combining PANDAseq²⁹ and QIIME 2 (<https://qiime2.org>).³⁰ After chimera removal, high-quality reads were clustered into amplicon sequence variants (ASVs) through an open-reference strategy performed with DADA2.³¹ Taxonomy was assigned using the vsearch classifier³² against Greengenes database as a reference (release: May 2013). Alpha diversity was measured using the metric phylogenetic diversity (PD) whole tree and Shannon and Simpson indices as well as by estimating the number of observed ASVs. Beta diversity was evaluated using the Bray–Curtis dissimilarity measure and visualized on a principal coordinate analysis plot. Heat plots and bar plots were built by means of the packages made4³³ and vegan (<http://www.cran.r-project.org/package=vegan>). The significance of separation among samples was tested by a permutation test with pseudo- F ratios using the function *adonis* in *vegan*. Statistics was performed using R Studio 1.0.44 on R software version 3.3.2 (<https://www.r-project.org/>) implemented with the packages *stats* and *vegan*. Significant associations between genus-level profiles were assessed by the Kendall correlation test, while differences in the relative abundance profiles between study groups were evaluated by the Kruskal–Wallis and Wilcoxon signed rank-sum test.

CAGs were identified as previously described.³⁴ In brief, associations among bacterial families, present in at least 20% of the samples with a relative abundance of >0.1%, were evaluated by the Kendall correlation test, displayed using hierarchical Ward clustering with the Spearman correlation-based distance metrics, and utilized to determine co-abundant groups of bacterial families. Significant associations were controlled for multiple testing using the q -value method (false discovery rate, FDR ≤ 0.05). Permutational MANOVA was used to determine whether the CAGs were significantly different from each other. Wiggum plot networks were created using the Cytoscape software (<http://www.cytoscape.org>), as previously reported.³⁵ The circle size represents the bacterial abundance or variations (T1–T0) and connections between nodes represent

positive or negative significant Kendall correlations between families (FDR \leq 0.05).

Methods for microbial mRNA sequence analysis were performed as previously described.³⁶ Briefly, reads were filtered for quality ($q < 20$) and contamination (human genome and rRNA) using the KneadData v0.3 pipeline (<http://huttenhower.sph.harvard.edu/kneaddata>) and the Human Microbiome Project (HMP) procedure,³⁷ which includes the Trimmomatic³⁸ and BMTagger³⁹ algorithms. Trimmed non-human reads shorter than 60 nt were discarded. Taxonomic profiling was performed using the MetaPhlan2 classifier.⁴⁰ Metatranscriptomes were functionally profiled using HUMAnN2³⁶ to quantify genes and pathways. Briefly, for each sample, taxonomic profiling was used to identify detectable organisms. Reads were recruited to sample-specific ChocoPhlan pangenomes including all gene families in any detected microbes using Bowtie2.⁴¹ Unmapped reads were aligned against UniRef90⁴² using DIAMOND translated search.⁴³ Hits were counted per gene family and normalized for length and alignment quality. The resulting table was transformed into a KEGG abundance table using the "humann2_regroup_table" command and the KO-Uniref90 mapping file. The final output was subsequently collapsed in a table of KO relative abundances, quantifying the corresponding transcripts of gene families in each sample. *P*-values were corrected for multiple comparisons using the Benjamini–Hochberg method when appropriate. *P*-values \leq 0.05 were considered statistically significant.

Drug Stability and Metabolite Analysis. Sample Preparation. An aliquot of the samples (50 μ L) was added with 150 μ L of cold acetonitrile to precipitate the protein content. The tube was vortex mixed for 30 s and centrifuged at 21,100g for 15 min at 4 °C. The supernatant was then transferred to LC–MS vials for analysis either as non-diluted or as further diluted 2-fold in mobile phase A.

Targeted LC-MS/MS Analysis: Degradation Profiles. The targeted analysis was performed on a Waters ACQUITY UPLC/MS TQD system consisting of a TQD (triple quadrupole detector) mass spectrometer equipped with an electrospray ionization interface and a photodiode array *e* λ Detector. Electrospray ionization (ESI) was applied in positive/negative mode. Compound-dependent parameters as multi-reaction monitoring (MRM) transitions and collision energy were developed for each compound as shown in Table S3.

Untargeted LC-MS/MS Analysis: Metabolite Identification. The untargeted analysis was performed on a Synapt G2 QTOF instrument coupled to an Acquity UPLC system (Waters Inc.). High-resolution MS and MS/MS spectra were acquired in either ESI+ or ESI- modes in a mass range of 50–1200 *m/z*. Tandem mass analysis was performed in MS^S mode using a linear ramp of collision energy (20–40 eV) in the trap region of the instrument. The scan time was set to 0.3 s. Spectra were real-time recalibrated by using leucine enkephalin (2 ng/ μ L) as the reference mass.

For both analyses, different chromatographic conditions (*e.g.*, mobile phases and columns) were used for each compound, but all separations were carried out at 45 °C at a flow rate of 0.45 mL/min.

Table S4 summarizes the analytical conditions used for each compound.

Data Analysis. In the targeted analysis, each drug in the MGM incubation was analyzed against the corresponding reference incubation (drug incubated under the same conditions in the same medium but in the absence of feces). The peak of the parent compound was integrated at all three time points (0, 24, and 48 h) to obtain the stability/degradation profile and to estimate the corresponding half-life.

In the untargeted analysis, the corresponding metabolites were identified by their accurate MS and MS/MS spectrum.

■ ASSOCIATED CONTENT

SI Supporting Information

The Supporting Information is available free of charge at <https://pubs.acs.org/doi/10.1021/acs.jmedchem.1c01333>.

Molecular formula strings for the 10 selected compounds (CSV)

Setup and optimization of the MGM screening platform, experimental analysis data regarding the gut microbiome composition and function in presence of the 10 selected compounds and DMSO, and analytical conditions for all compounds (PDF)

■ AUTHOR INFORMATION

Corresponding Author

Marco Candela – Department of Pharmacy and Biotechnology, University of Bologna, Bologna 40126, Italy; orcid.org/0000-0001-7420-790X; Email: marco.candela@unibo.it

Authors

Monica Barone – Department of Medical and Surgical Sciences, University of Bologna, Bologna 40138, Italy; orcid.org/0000-0001-5229-570X

Simone Rampelli – Department of Pharmacy and Biotechnology, University of Bologna, Bologna 40126, Italy

Elena Biagi – Department of Pharmacy and Biotechnology, University of Bologna, Bologna 40126, Italy

Sine Mandrup Bertozzi – Analytical Chemistry Lab, Istituto Italiano di Tecnologia, Genova 16163, Italy

Federico Falchi – Molecular Horizon, Bettona (PG) 06084, Italy

Andrea Cavalli – Department of Pharmacy and Biotechnology, University of Bologna, Bologna 40126, Italy; Computational & Chemical Biology, Istituto Italiano di Tecnologia, Genova 16163, Italy; orcid.org/0000-0002-6370-1176

Andrea Armirotti – Analytical Chemistry Lab, Istituto Italiano di Tecnologia, Genova 16163, Italy; orcid.org/0000-0002-3766-8755

Patrizia Brigidi – Department of Medical and Surgical Sciences, University of Bologna, Bologna 40138, Italy

Silvia Turroni – Department of Pharmacy and Biotechnology, University of Bologna, Bologna 40126, Italy

Complete contact information is available at: <https://pubs.acs.org/10.1021/acs.jmedchem.1c01333>

Author Contributions

#M.B. and S.R. contributed equally to the work.

Notes

The authors declare no competing financial interest.

■ ABBREVIATIONS USED

ASVs, amplicon sequence variants; BMI, body mass index; CAGs, co-abundance groups; ESI, electrospray ionization; FDR, false discovery rate; GM, gut microbiome; HMP, Human Microbiome Project; MGM, mini gut model; MRM, multi-reaction monitoring; MW, molecular weight; OD, optical density

■ REFERENCES

- (1) Schmidt, T. S. B.; Raes, J.; Bork, P. The human gut microbiome: From association to modulation. *Cell* **2018**, *172*, 1198–1215.
- (2) Jackson, M. A.; Verdi, S.; Maxan, M. E.; Shin, C. M.; Zierer, J.; Bowyer, R. C. E.; Martin, T.; Williams, F. M. K.; Menni, C.; Bell, J. T.; Spector, T. D.; Steves, C. J. Gut microbiota associations with common diseases and prescription medications in a population-based cohort. *Nat. Commun.* **2018**, *9*, 2655.
- (3) Durack, J.; Lynch, S. V. The gut microbiome: Relationships with disease and opportunities for therapy. *J Exp Med* **2019**, *216*, 20–40.

- (4) Jia, W.; Li, H.; Zhao, L.; Nicholson, J. K. Gut microbiota: a potential new territory for drug targeting. *Nat Rev Drug Discov* **2008**, *7*, 123–129.
- (5) Wilson, I. D.; Nicholson, J. K. Gut microbiome interactions with drug metabolism, efficacy, and toxicity. *Transl Res* **2017**, *179*, 204–222.
- (6) Duvallet, C.; Gibbons, S. M.; Gurry, T.; Irizarry, R. A.; Alm, E. J. Meta-analysis of gut microbiome studies identifies disease-specific and shared responses. *Nat. Commun.* **2017**, *8*, 1784.
- (7) Suez, J.; Elinav, E. The path towards microbiome-based metabolite treatment. *Nat Microbiol* **2017**, *2*, 1.
- (8) Reardon, S. Microbiome therapy gains market traction. *Nature* **2014**, *509*, 269–270.
- (9) Turrone, S.; Brigidi, P.; Cavalli, A.; Candela, M. Microbiota-host transgenomic metabolism, bioactive molecules from the inside. *J. Med. Chem.* **2018**, *61*, 47–61.
- (10) Falony, G.; Joossens, M.; Vieira-Silva, S.; Wang, J.; Darzi, Y.; Faust, K.; Kurilshikov, A.; Bonder, M. J.; Valles-Colomer, M.; Vandeputte, D.; Tito, R. Y.; Chaffron, S.; Rymenans, L.; Verspecht, C.; De Sutter, L.; Lima-Mendez, G.; D'hoel, K.; Jonckheere, K.; Homola, D.; Garcia, R.; Tigchelaar, E. F.; Eeckhaert, L.; Fu, J.; Henckaerts, L.; Zhernakova, A.; Wijmenga, C.; Raes, J. Population-level analysis of gut microbiome variation. *Science* **2016**, *352*, 560–564.
- (11) Maier, L.; Pruteanu, M.; Kuhn, M.; Zeller, G.; Telzerow, A.; Anderson, E. E.; Brochado, A. R.; Fernandez, K. C.; Dose, H.; Mori, H.; Patil, K. R.; Bork, P.; Typas, A. Extensive impact of non-antibiotic drugs on human gut bacteria. *Nature* **2018**, *555*, 623–628.
- (12) Spanogiannopoulos, P.; Turnbaugh, P. J. Broad collateral damage of drugs against the gut microbiome. *Nat. Rev. Gastroenterol. Hepatol.* **2018**, *15*, 457–458.
- (13) Rettedal, E. A.; Gumpert, H.; Sommer, M. O. A. Cultivation-based multiplex phenotyping of human gut microbiota allows targeted recovery of previously uncultured bacteria. *Nat. Commun.* **2014**, *5*, 4714.
- (14) Tramontano, M.; Andrejev, S.; Pruteanu, M.; Klünemann, M.; Kuhn, M.; Galardini, M.; Jouhten, P.; Zelezniak, A.; Zeller, G.; Bork, P.; Typas, A.; Patil, K. R. Nutritional preferences of human gut bacteria reveal their metabolic idiosyncrasies. *Nat. Microbiol.* **2018**, *3*, 514–522.
- (15) Ejim, L.; Farha, M. A.; Falconer, S. B.; Wildenhain, J.; Coombes, B. K.; Tyers, M.; Brown, E. D.; Wright, G. D. Combinations of antibiotics and nonantibiotic drugs enhance antimicrobial efficacy. *Nat. Chem. Biol.* **2011**, *7*, 348–350.
- (16) David, L. A.; Maurice, C. F.; Carmody, R. N.; Gootenberg, D. B.; Button, J. E.; Wolfe, B. E.; Ling, A. V.; Devlin, A. S.; Varma, Y.; Fischbach, M. A.; Biddinger, S. B.; Dutton, R. J.; Turnbaugh, P. J. Diet rapidly and reproducibly alters the human gut microbiome. *Nature* **2014**, *505*, 559–563.
- (17) Bedarf, J. R.; Hildebrand, F.; Coelho, L. P.; Sunagawa, S.; Bahram, M.; Goesser, F.; Bork, P.; Willner, U. Functional implications of microbial and viral gut metagenome changes in early stage L-DOPA-naive Parkinson's disease patients. *Genome Med.* **2017**, *9*, 39.
- (18) Berer, K.; Gerdes, L. A.; Cekanaviciute, E.; Jia, X.; Xiao, L.; Xia, Z.; Liu, C.; Klotz, L.; Stauffer, U.; Baranzini, S. E.; Kumpfel, T.; Hohlfeld, R.; Krishnamoorthy, G.; Wekerle, H. Gut microbiota from multiple sclerosis patients enables spontaneous autoimmune encephalomyelitis in mice. *Proc. Natl. Acad. Sci. U. S. A.* **2017**, *114*, 10719–10724.
- (19) Cekanaviciute, E.; Yoo, B. B.; Runia, T. F.; Debelius, J. W.; Singh, S.; Nelson, C. A.; Kanner, R.; Bencosme, Y.; Lee, Y. K.; Hauser, S. L.; Crabtree-Hartman, E.; Sand, I. K.; Gacias, M.; Zhu, Y.; Casaccia, P.; Cree, B. A. C.; Knight, R.; Mazmanian, S. K.; Baranzini, S. E. Gut bacteria from multiple sclerosis patients modulate human T cells and exacerbate symptoms in mouse models. *Proc. Natl. Acad. Sci. U. S. A.* **2017**, *114*, 10713–10718.
- (20) Scheiman, J.; Lubert, J. M.; Chavkin, T. A.; MacDonald, T.; Tung, A.; Pham, L. D.; Wibowo, M. C.; Wurth, R. C.; Punthambaker, S.; Tierney, B. T.; Yang, Z.; Hattab, M. W.; Avila-Pacheco, J.; Clish, C. B.; Lessard, S.; Church, G. M.; Kostic, A. D. Meta-omics analysis of elite athletes identifies a performance-enhancing microbe that functions via lactate metabolism. *Nat. Med.* **2019**, *25*, 1104–1109.
- (21) Carbonero, F.; Benefiel, A. C.; Alizadeh-Ghamsari, A. H.; Gaskins, H. R. Microbial pathways in colonic sulfur metabolism and links with health and disease. *Front. Physiol.* **2012**, *3*, 448.
- (22) Hughes, H. K.; Rose, D.; Ashwood, P. The gut microbiota and dysbiosis in autism spectrum disorders. *Curr. Neurol. Neurosci. Rep.* **2018**, *18*, 81.
- (23) Martinez, C.; Antolin, M.; Santos, J.; Torrejon, A.; Casellas, F.; Borrue, N.; Guarner, F.; Malagelada, J. R. Unstable composition of the fecal microbiota in ulcerative colitis during clinical remission. *Am. J. Gastroenterol.* **2008**, *103*, 643–648.
- (24) Rowan, F.; Docherty, N. G.; Murphy, M.; Murphy, B.; Calvin Coffey, J.; O'Connell, P. R. *Desulfovibrio* bacterial species are increased in ulcerative colitis. *Dis. Colon Rectum* **2010**, *53*, 1530–1536.
- (25) Duan, J.; Dixon, S. L.; Lowrie, J. F.; Sherman, W. Analysis and comparison of 2D fingerprints: insights into database screening performance using eight fingerprint methods. *J. Mol. Graphics Modell.* **2010**, *29*, 157–170.
- (26) Sastry, M.; Lowrie, J. F.; Dixon, S. L.; Sherman, W. Large-scale systematic analysis of 2D fingerprint methods and parameters to improve virtual screening enrichments. *J. Chem. Inf. Model.* **2010**, *50*, 771–784.
- (27) Yu, Z.; Morrison, M. Improved extraction of PCR-quality community DNA from digesta and fecal samples. *BioTechniques* **2004**, *36*, 808–812.
- (28) Barone, M.; Turrone, S.; Rampelli, S.; Soverini, M.; D'Amico, F.; Biagi, E.; Brigidi, P.; Troiani, E.; Candela, M. Gut microbiome response to a modern Paleolithic diet in a Western lifestyle context. *PLoS One* **2019**, *14*, e0220619.
- (29) Masella, A. P.; Bartram, A. K.; Truszkowski, J. M.; Brown, D. G.; Neufeld, J. D. PANDaseq: paired-end assembler for illumina sequences. *BMC Bioinf.* **2012**, *13*, 31.
- (30) Bolyen, E.; Rideout, J. R.; Dillon, M. R.; Bokulich, N. A.; Abnet, C. C.; Al-Ghalith, G. A.; Alexander, H.; Alm, E. J.; Arumugam, M.; Asnicar, F.; Bai, Y.; Bisanz, J. E.; Bittinger, K.; Brejnrod, A.; Brislawn, C. J.; Brown, C. T.; Callahan, B. J.; Caraballo-Rodriguez, A. M.; Chase, J.; Cope, E. K.; Da Silva, R.; Diener, C.; Dorrestein, P. C.; Douglas, G. M.; Durall, D. M.; Duvallet, C.; Edwards, C. F.; Ernst, M.; Estaki, M.; Fouquier, J.; Gauglitz, J. M.; Gibbons, S. M.; Gibson, D. L.; Gonzalez, A.; Gorlick, K.; Guo, J.; Hillmann, B.; Holmes, S.; Holste, H.; Huttenhower, C.; Huttley, G. A.; Janssen, S.; Jarmusch, A. K.; Jiang, L.; Kaehler, B. D.; Kang, K. B.; Keefe, C. R.; Keim, P.; Kelley, S. T.; Knights, D.; Koester, I.; Kosciulek, T.; Kreps, J.; Langille, M. G. I.; Lee, J.; Ley, R.; Liu, Y. X.; Loftfield, E.; Lozupone, C.; Maher, M.; Marotz, C.; Martin, B. D.; McDonald, D.; McIver, L. J.; Melnik, A. V.; Metcalf, J. L.; Morgan, S. C.; Morton, J. T.; Naimey, A. T.; Navas-Molina, J. A.; Nothias, L. F.; Orchanian, S. B.; Pearson, T.; Peoples, S. L.; Petras, D.; Preuss, M. L.; Pruesse, E.; Rasmussen, L. B.; Rivers, A.; Robeson, M. S., II; Rosenthal, P.; Segata, N.; Shaffer, M.; Shiffer, A.; Sinha, R.; Song, S. J.; Spear, J. R.; Swafford, A. D.; Thompson, L. R.; Torres, P. J.; Trinh, P.; Tripathi, A.; Turnbaugh, P. J.; Ul-Hasan, S.; van der Hooft, J. J. J.; Vargas, F.; Vazquez-Baeza, Y.; Vogtmann, E.; von Hippel, M.; Walters, W.; Wan, Y.; Wang, M.; Warren, J.; Weber, K. C.; Williamson, C. H. D.; Willis, A. D.; Xu, Z. Z.; Zaneveld, J. R.; Zhang, Y.; Zhu, Q.; Knight, R.; Caporaso, J. G. Reproducible, interactive, scalable and extensible microbiome data science using QIIME 2. *Nat. Biotechnol.* **2019**, *37*, 852–857.
- (31) Callahan, B. J.; McMurdie, P. J.; Rosen, M. J.; Han, A. W.; Johnson, A. J. A.; Holmes, S. P. DADA2: High-resolution sample inference from illumina amplicon data. *Nat. Methods* **2016**, *13*, 581–583.
- (32) Rognes, T.; Flouri, T.; Nichols, B.; Quince, C.; Mahé, F. VSEARCH: A versatile open source tool for metagenomics. *PeerJ* **2016**, *4*, e2584.

- (33) Culhane, A. C.; Thioulouse, J.; Perriere, G.; Higgins, D. G. MADE4: an R package for multivariate analysis of gene expression data. *Bioinformatics* **2005**, *21*, 2789–2790.
- (34) Rampelli, S.; Guenther, K.; Turrone, S.; Wolters, M.; Veidebaum, T.; Kourides, Y.; Molnár, D.; Lissner, L.; Benitez-Paez, A.; Sanz, Y.; Fraterman, A.; Michels, N.; Brigidi, P.; Candela, M.; Ahrens, W. Pre-obese children's dysbiotic gut microbiome and unhealthy diets may predict the development of obesity. *Commun. Biol.* **2018**, *1*, 222.
- (35) Shannon, P.; Markiel, A.; Ozier, O.; Baliga, N. S.; Wang, J. T.; Ramage, D.; Amin, N.; Schwikowski, B.; Ideker, T. Cytoscape: a software environment for integrated models of biomolecular interaction networks. *Genome Res.* **2003**, *13*, 2498–2504.
- (36) Franzosa, E. A.; McIver, L. J.; Rahnavard, G.; Thompson, L. R.; Schirmer, M.; Weingart, G.; Lipson, K. S.; Knight, R.; Caporaso, J. G.; Segata, N.; Huttenhower, C. Species-level functional profiling of metagenomes and metatranscriptomes. *Nat. Methods* **2018**, *15*, 962–968.
- (37) Turnbaugh, P. J.; Ley, R. E.; Hamady, M.; Fraser-Liggett, C. M.; Knight, R.; Gordon, J. I. The human microbiome project. *Nature* **2007**, *449*, 804–810.
- (38) Bolger, A. M.; Lohse, M.; Usadel, B. Trimmomatic: a flexible trimmer for Illumina sequence data. *Bioinformatics* **2014**, *30*, 2114–2120.
- (39) Lee, P. H.; Shatkay, H. BNTagger: improved tagging SNP selection using Bayesian networks. *Bioinformatics* **2006**, *22*, e211–e219.
- (40) Truong, D. T.; Franzosa, E. A.; Tickle, T. L.; Scholz, M.; Weingart, G.; Pasolli, E.; Tett, A.; Huttenhower, C.; Segata, N. MetaPhlan2 for enhanced metagenomic taxonomic profiling. *Nat. Methods* **2015**, *12*, 902–903.
- (41) Langdon, W. B. Performance of genetic programming optimised Bowtie2 on genome comparison and analytic testing (GCAT) benchmarks. *BioData Min.* **2015**, *8*, 1.
- (42) Suzek, B. E.; Wang, Y.; Huang, H.; McGarvey, P. B.; Wu, C. H.; UniProt Consortium. UniRef clusters: a comprehensive and scalable alternative for improving sequence similarity searches. *Bioinformatics* **2015**, *31*, 926–932.
- (43) Buchfink, B.; Xie, C.; Huson, D. H. Fast and sensitive protein alignment using DIAMOND. *Nat. Methods* **2015**, *12*, 59–60.